



## Short communication

Long cycle-life LiFePO<sub>4</sub>/Cu-Sn lithium ion battery using foam-type three-dimensional current collectorMasaru Yao<sup>a,\*</sup>, Kazuki Okuno<sup>b</sup>, Tsutomu Iwaki<sup>a</sup>, Tomoyuki Awazu<sup>b</sup>, Tetsuo Sakai<sup>a,\*\*</sup><sup>a</sup> National Institute of Advanced Industrial Science and Technology, Midorigaoka, Ikeda, Osaka 563-8577, Japan<sup>b</sup> Sumitomo Electric Industries Ltd., Koyakita, Itami, Hyogo 664-0016, Japan

## ARTICLE INFO

## Article history:

Received 23 July 2009

Received in revised form 6 October 2009

Accepted 7 October 2009

Available online 8 November 2009

## Keywords:

Long cycle-life

Three-dimensional current collector

Cu-Sn alloy electrode

LiFePO<sub>4</sub>

Aqueous slurry

## ABSTRACT

To improve the cycle-life performance of LiFePO<sub>4</sub>/Cu-Sn lithium ion battery, a new methodology using a foam-type three-dimensional current collector was investigated. By applying the three-dimensional nickel substrate for the negative electrode, instead of conventional copper foil, the cycle performance of the Cu-Sn electrode was improved. In addition, a heat treatment of the electrode was revealed to suppress the capacity decline drastically: the heat treated electrode showed the capacity above 400 mAh g<sup>-1</sup> even after 50 cycles. A full-cell which combined the developed negative electrode and a positive electrode based on LiFePO<sub>4</sub> also showed a favorable cycle performance. Furthermore, a full-cell using aqueous slurry was prepared, and the cell exhibited an excellent cycle-life performance in which it maintained above 90% of the maximum capacity even at the 200th cycle.

© 2009 Elsevier B.V. All rights reserved.

## 1. Introduction

Lithium ion batteries using lithium cobalt oxide (LiCoO<sub>2</sub>) and graphite-based materials for the positive and negative electrodes, respectively, have been widely used as electric power sources. To increase the energy density of the batteries, various materials have been studied. As new negative active materials, some metallic substances which form alloys with lithium have been evaluated [1,2], and especially, tin-based alloys have been extensively studied because of the low toxicity and the large specific capacity [3–8]. Tin reacts with lithium forming the alloy Li<sub>4.4</sub>Sn and its theoretical capacity is about 1000 mAh g<sup>-1</sup> which is about three-times larger than that of the conventional graphite-based materials. However, the tin-based negative electrodes generally exhibit poor cycle-life performances. During the charge/discharge processes, the tin-based active materials cause a large volumetric change followed by the pulverization of the active materials powder, which leads to the capacity fading. To suppress the volumetric change, some methodologies have been attempted, such as alloy-formations of tin with a various electrochemically inert metal [2–4], carbon-deposition [5,6], and structure-control of active material layer [7,8].

As another methodology, we hereby propose a new strategy using a foam-type three-dimensional (3D) substrate instead of the foil-type current collectors which have been generally used. Whereas this kind of 3D substrate has been used as a current collector for the positive electrode of nickel/metal-hydride (Ni/MH) batteries, there has been little attention paid for the current collectors of lithium ion batteries [9]. We have extensively studied the effect of the current collector structure on some electrochemical energy storage systems [10–16], and have previously revealed a benefit of the 3D substrate use for improving the power output property of a positive electrode of lithium ion batteries [16]. In this paper, the tin-based negative electrodes using the 3D substrate and the full-cells using the 3D substrates for positive and negative electrodes were prepared and the effect of the 3D substrate on the cycle-life performance was examined. Furthermore, the applicability of aqueous slurry for LiFePO<sub>4</sub>/Cu-Sn battery system was investigated.

## 2. Experimental

As a 3D current collector, a foam-type nickel substrate was used (Celmet No. 8, Sumitomo Electric Industries Ltd.). This substrate is manufactured by nickel plating on foamed polyurethane followed by a heat treatment to remove the inner polyurethane. The morphology of the 3D substrate was examined with a digital microscope (VHX-200, Keyence Corp.). Analytical data of the substrate such as weight, thickness, porosity, and specific surface area were 420 g m<sup>-2</sup>, 1.4 mm, 97%, 5800 m<sup>2</sup> m<sup>-3</sup>, respectively.

\* Corresponding author at: Research Team of Secondary Battery System, National Institute of Advanced Industrial Science and Technology (AIST) Kansai, 1-8-31 Midorigaoka, Ikeda, Osaka 563-8577, Japan. Tel.: +81 72 751 9653; fax: +81 72 751 9629.

\*\* Corresponding author. Tel.: +81 72 751 9611; fax: +81 72 751 9623.

E-mail addresses: [m.yao@aist.go.jp](mailto:m.yao@aist.go.jp) (M. Yao), [sakai-tetsuo@aist.go.jp](mailto:sakai-tetsuo@aist.go.jp) (T. Sakai).

As a tin-based material, Cu–Sn alloy powder (Sn content: 35 wt%) was used which was provided by Fukuda Metal Foil & Powder Co. Ltd. [4]. Slurry for the negative electrode was prepared by mixing the alloy powder, ketchen black (KB) as a conductive additive, and polyvinylidene fluoride (PVDF) as a binder in a weight ratio of 85:5:15 with the organic solvent of *N*-methyl-2-pyrrolidone (NMP). The prepared slurry was loaded into the 3D substrates; and the resultant electrodes were dried and then roll-pressed to the thickness of about 90  $\mu\text{m}$ . In addition, some electrodes were annealed at 500 °C for 8 h under vacuum. For a comparison, a conventional electrode was also prepared by using copper foil as the current collector (electrode thickness: 50  $\mu\text{m}$ ). Each prepared negative electrodes was prepared such that they have approximately the same capacity. The prepared each electrode was placed into an R2032 coin type cell case with a glass filter, porous polypropylene separator (Celgard No. 2400, Celgard Inc.), and a lithium sheet as a counter electrode. After an electrolyte of the mixed solution of ethylene carbonate and diethyl carbonate containing lithium hexafluorophosphate (1.0 mol L<sup>-1</sup> LiPF<sub>6</sub> in EC/DEC = 1/1) was added, the half-cell case was sealed.

For the full-cells composed of both the negative and positive electrodes, carbon layer deposited lithium iron phosphate (LiFePO<sub>4</sub>) (primary particle diameter: 70–100 nm) (Mitsui Engineering & Shipbuilding Co. Ltd. [17]) was used as the positive active material. For this positive electrode, a high tolerance nickel-chromium (Ni–Cr) 3D substrate was used [13,16]. For the negative electrode, the above-mentioned annealing process was applied under vacuum and then pre-doped by using lithium metal to cover the irreversible capacity of the alloy-based active materials [18]. Specifically, this pre-doping was carried out as follows. The required amount of lithium for irreversible capacity was estimated first from the experimental result obtained from the initial charge/discharge curves of each negative electrode. The predetermined total amount of lithium sheet was then placed in contact with the surface of each electrode before assembling the cell. After the electrolyte was added, the prepared cell was left as it is till the open-circuit-voltage becomes stable. The other materials used for assembling the full-cells were the same to those of the half-cells. The capacity of the positive electrode was about half as large as that of the negative electrode. For a comparison, a conventional full-cell was also prepared by using an aluminum foil and a copper foil for the positive and the negative current collector, respectively.

The full-cell using aqueous slurry for the both positive and negative electrodes was also examined. Aqueous solution of carboxymethylcellulose (CMC) (Daicel Chemical Industries Ltd.) and aqueous dispersion of poly-tetrafluoroethylene (PTFE) (Daikin Industries Ltd.) as the binder materials were used instead the organic solution of PVDF in NMP. The aqueous slurry was prepared by mixing the active material powder, the conductive additive, and the above-mentioned aqueous solution in a specific weight ratio with water (LiFePO<sub>4</sub> powder:KB:CMC:PTFE = 90:5:4:1 for the positive electrode; Cu–Sn powder:KB:CMC = 93:6:1 for the negative electrode, where PTFE was not used). The both electrodes were prepared by loading the aqueous slurries into the 3D substrates followed by the roll-press. For these electrodes, a careful drying process at the temperature of over 150 °C under vacuum was carried out to remove the water enough. Subsequently, the annealing process for the negative electrode was applied under vacuum and then pre-doped by using a lithium metal sheet. The cell was assembled in the similar way described above.

In the cycle-life test, the prepared half-cells were galvanostatically charged at a current density of 100 mA g<sup>-1</sup> followed by a potentiostatic charge at 0.0 V vs. Li<sup>+</sup>/Li for 2 h; then, they were galvanostatically discharged at a current density of 100 mA g<sup>-1</sup> with a cutoff voltage of 1.0 V vs. Li<sup>+</sup>/Li (In this paper, the charge and discharge represent lithiation and delithiation processes on the alloy,

respectively). In the cycle-life test of the full-cells, the cells were galvanostatically charged and discharged at the current density of 0.2-C rate, where *n*-C corresponds to the current density to complete charging or discharging of the cell in 1/*n* hours. All of the charge/discharge tests were performed at 30 °C with a computer-controlled charge/discharge system (BLS series, Keisokuki Center Co. Ltd.).

### 3. Results and discussion

Fig. 1 shows an optical microscopic image of the 3D substrate. The morphology of the substrate reflects the structure of the foamed polyurethane grounding. The 3D substrate has a large surface area due to its unique framework structure. The active material particles can be filled in the inner pore space. This characteristic structure could suppress the separation of the active materials from the current collectors caused by the large volumetric change of the active material powder during the charge/discharge process.

Fig. 2 shows a comparison of the charge/discharge curves of the prepared Cu–Sn-based negative electrodes at the second cycle. All of the electrodes show large capacity about 500 mA h g<sup>-1</sup>. These obtained initial discharge capacities are typical values for Cu–Sn materials [2–7]. The electrode using the conventional copper foil and the one using the 3D substrate exhibit almost the same behavior in which the discharge curves have two plateau voltage regions at 0.5 and 0.7 V (vs. Li<sup>+</sup>/Li). This attributes to the charge/discharge process of Cu<sub>6</sub>Sn<sub>5</sub> phase [3,4]. On the other hand, the annealed electrode exhibits a smooth discharge curve having one plateau region.

The cycle-life performance of the prepared Cu–Sn-based negative electrodes is shown in Fig. 3. The capacity retention ratios at the 50th cycle of the electrodes were 24, 55 and 92% for the conventional electrode, the electrode using the 3D substrate and the annealed electrode using the 3D substrate, respectively. By only applying the 3D substrate to the negative electrode, the capacity decrease was suppressed to some extent. Moreover, the additional annealing treatment showed a significant effect to improve the cycle-life performance. Annealing temperature was also examined, and the annealing at 500 °C showed the best cycle-life performance among the temperatures we checked. Contrary, the annealing treat-

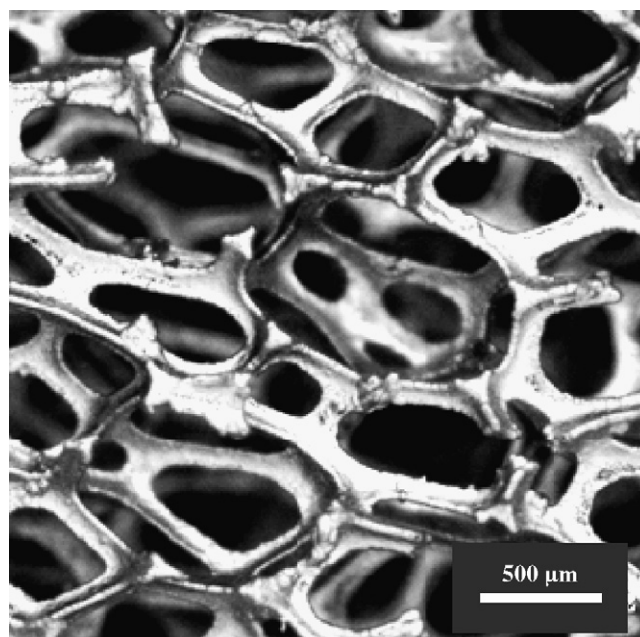
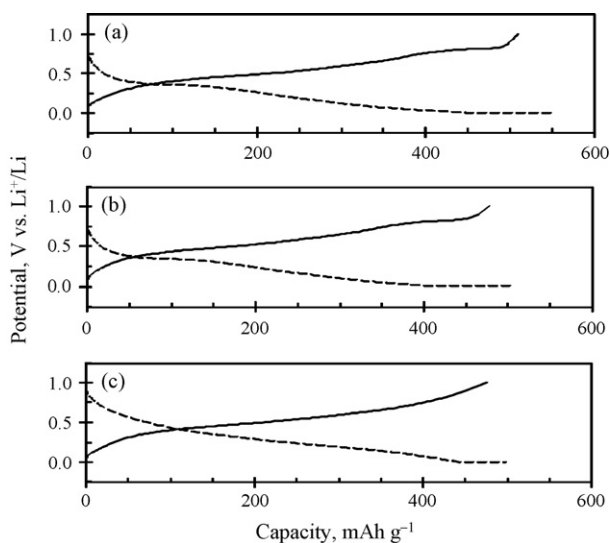


Fig. 1. Optical microscopic image of the 3D substrate.



**Fig. 2.** Charge/discharge curves of the negative electrodes at the second cycles: (a) the electrode using the Cu-foil, (b) the electrode using the 3D substrate, and (c) the annealed electrode using the 3D substrate. Current densities of  $100 \text{ mA g}^{-1}$  were applied for the both charge and discharge.

ment on the conventional electrode using Cu-foil did not provide such a significant improvement.

In order to investigate the property of the annealed negative electrode in a practical system, a full-cell was assembled with a positive electrode using carbon layer deposited  $\text{LiFePO}_4$  as active material. For the positive electrode, a 3D substrate made out of nickel-chromium (Ni-Cr) alloy was used to suppress the corrosion due to the high electric potential of the cell [13,16]. This Ni-Cr 3D substrate was manufactured by alloying the nickel 3D substrate with metallic chromium powder, and the substrate has a passivation layer on the surface, which makes the electrochemical tolerance much higher than that of pure nickel substrate.

In general, alloy-based electrodes show large irreversible capacity as described in Section 2. Owing to this irreversible capacity, one cannot use these alloy-based negative active materials as is. To overcome this problem, we applied a pre-doping technique

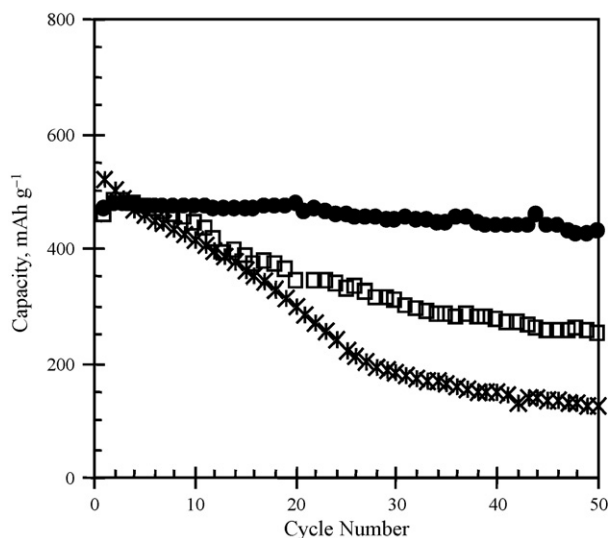


**Fig. 3.** Cycle-life performance of the Cu-Sn electrodes at  $30^\circ\text{C}$  (current density:  $100 \text{ mA g}^{-1}$ , potential range:  $0.0\text{--}1.0 \text{ V vs. Li}^+/\text{Li}$ ). (●: annealed electrode using the 3D substrate; □: electrode using the 3D substrate; \*: electrode using conventional Cu-foil.)

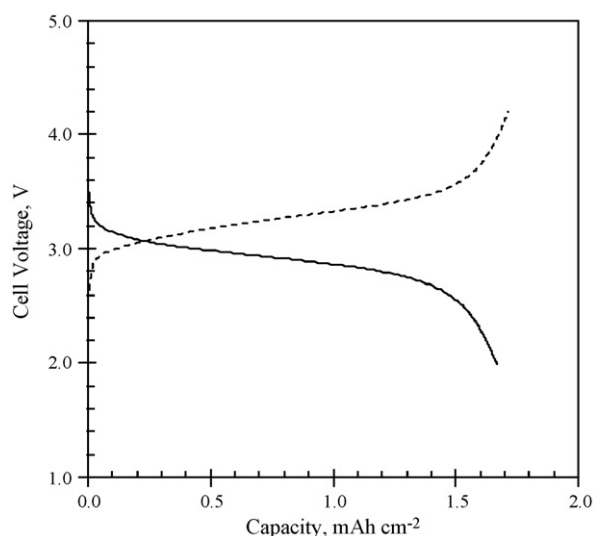


**Fig. 4.** Charge/discharge curves of the full-cell using the 3D substrates for the both positive and negative electrodes at the fifth cycle. The negative electrode was annealed before the assembling the cell. (Current density:  $0.2\text{-C}$  rate, potential range:  $2.0\text{--}4.2 \text{ V}$ , temperature:  $30^\circ\text{C}$ .)

using a lithium metal sheet for the negative electrode before use [18].

Fig. 4 shows the charge and discharge curves of the prepared full-cell using the 3D substrates for the both positive and negative electrodes at the current density of  $0.2\text{-C}$  rate. The cell shows the average discharge voltage of about  $2.8 \text{ V}$  at the early cycle, which approximately corresponds to the average potential difference between  $\text{LiFePO}_4$  electrode ( $\sim 3.4 \text{ V vs. Li}^+/\text{Li}$ ) and Cu-Sn-based electrode ( $\sim 0.6 \text{ V vs. Li}^+/\text{Li}$ ).

The cycle test was also carried out for the prepared full-cells at the same current density. Fig. 5 shows the comparison of the cycle-life performance of the full-cell using the 3D substrates and the full-cell using the conventional foil substrates. The discharge capacity of the full-cell using conventional foil substrates begins to decrease drastically from around the 15th cycle and falls to 2% of the initial capacity at the 100th cycle. On the other hand, the full-cell using the 3D substrates shows a much better cycle performance;

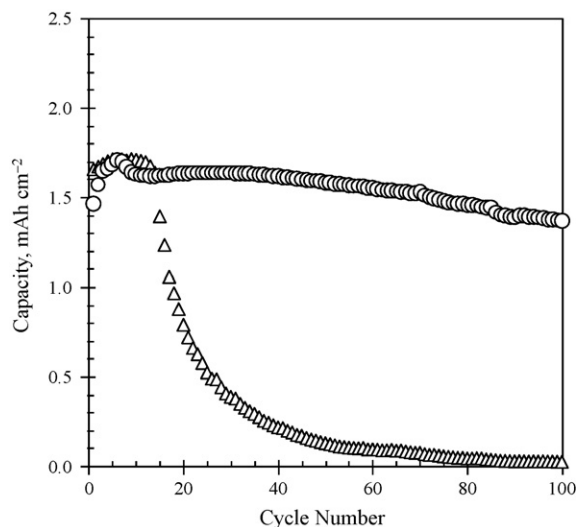


**Fig. 5.** Cycle-life performance of the full-cells at  $30^\circ\text{C}$  (Current density:  $0.2\text{-C}$  rate, potential range:  $2.0\text{--}4.2 \text{ V}$ ). (○: the full-cell using the 3D substrates for both the positive and annealed negative electrodes; △: the full-cell using conventional Al-foil and Cu-foil for the positive and negative electrodes, respectively.)

it maintains about an 80% of the initial capacity even after the 100 cycles. The high retention ability of the 3D substrate for the active material is considered to suppress the poor electrical contact which is often caused by the swelling of active material particles during the charge/discharge process. Besides, the annealing treatment of the electrode was found to be effective to improve the cycle-life property of the Cu-Sn electrode.

In a preliminary X-ray diffraction (XRD) measurement, the annealed electrode showed a complicated pattern composed of many peaks ascribed to partial oxidation, phase changes of the active material and alloys formation between the Cu-Sn powder and the nickel substrate. There are some reports on the improved cycle stability of tin-based electrode by oxidation [19–22]. For these oxidized materials such as SnO and SnO<sub>2</sub>, the lithium oxide matrix formed during the first charge works as a buffer for the volumetric change of the active material powder. On the other hand, an alloy formation of tin with nickel of substrate can also improve the cycle stability as negative active materials. Osaka and co-workers have reported the electrochemical properties of various Ni-Sn alloys [23,24]. In their studies, the alloy formation of tin with nickel is revealed to lead a stable cycle-life performance. In our case, similar alloys can form at the interface of alloy powder and the nickel substrate. In addition, the ternary alloy formation among copper, nickel and tin can also occur during the annealing process. Lots of phases are known for this ternary system [25–27], which will make the XRD pattern of the annealed electrode complex. The mechanism of the structural change during the annealing of the negative electrode is not clear at the present stage; however, the enhanced contact between the 3D substrate and the Cu-Sn powder upon heating, and the phase change itself are considered to synergistically work for the improvement in the cycle-life of the Cu-Sn-based negative electrode. In order to clarify the mechanism, a further investigation of the structure change of the alloy is under progress.

Finally, the applicability of aqueous slurry for the 3D substrate will be described. In the preparation process of electrodes of lithium ion batteries, organic solvent such as NMP is generally used for the slurry of active material powder. If the application of aqueous slurry becomes possible, the manufacturing process of the batteries can be simplified and reduce environmental load. However, the application of aqueous slurry is a challenging task because the binder materials used for aqueous slurry usually have some problems in such dispersion property, adhesibility, and wettability compared with these properties of the conventional binder materials used for organic slurry. In particular, the application of aqueous slurry for positive electrode is difficult because most aqueous binder has a problem in electrochemical stability at the high potential of lithium ion batteries. As shown in the results above, the electrodes using the 3D substrates exhibit favorable battery performances. The high retention ability of the 3D substrate for the active material could compensate the drawback of the low adhesibility of aqueous slurry system. We also prepared a full-cell by using aqueous slurry for both of the positive and negative electrodes. Specifically, CMC-PTFE/water or CMC/water-based slurry was used, instead of the conventional PVDF/NMP-based slurry. Fig. 6 shows charge and discharge curves of the prepared full-cell using the aqueous slurry at the current density of 0.2-C rate. The cell shows almost the same pattern to the cell using the conventional organic solvent-based slurry shown in Fig. 4. The cell exhibited an excellent cycle performance as shown in Fig. 7. The capacity increased, reached a maximum at around the 20th cycle, and then slightly decreased; however, the cell maintained more than 90% capacity of the maximum value even at the 200th cycle. The application of the 3D substrate was revealed to make the use of aqueous slurry possible for both of the negative and positive electrodes. It is particularly notable that popular binder material of PTFE becomes practicable for LiFePO<sub>4</sub> positive electrode by using the Ni-Cr 3D substrate since

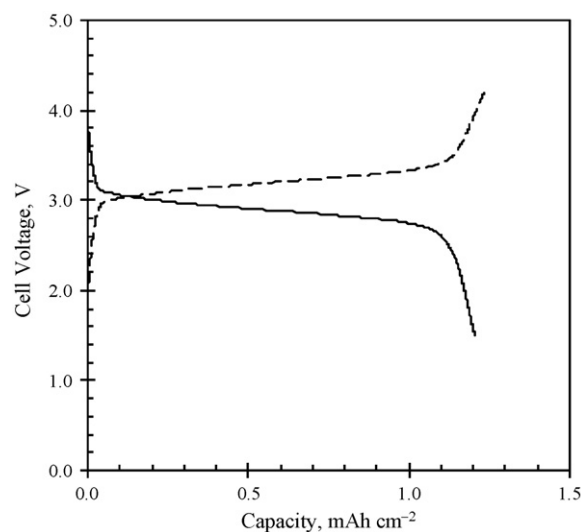


**Fig. 6.** Charge/discharge curves of the full-cell using the aqueous slurry at the 20th cycle. The 3D substrates were applied for both the positive and negative electrodes. The negative electrode was annealed before the assembling the cell. (Current density: 0.2-C rate, potential range: 1.5–4.2 V, temperature: 30 °C.)

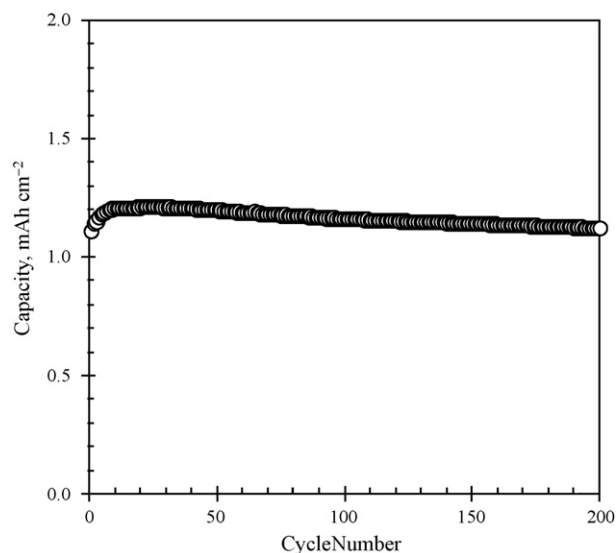


**Fig. 7.** Cycle-life performance of the full-cell using the aqueous slurry. The 3D substrates were applied for both the positive and negative electrodes. (Current density: 0.2-C rate, potential range: 1.5–4.2 V, temperature: 30 °C.)

the report on the use of aqueous slurry for positive electrode is only a few because of some drawbacks as described above. By replacing the organic slurry to aqueous one, the manufacturing process of lithium ion batteries becomes simple, which would lead to the reduction of environmental load.

#### 4. Conclusion

A new methodology using a 3D current collector was investigated, and was revealed to improve the charge/discharge performance of the Cu-Sn-based negative electrode of the lithium ion battery. The cycle-life performance was improved more by an annealing of the negative electrode at 500 °C under vacuum.

Furthermore, aqueous slurry becomes practicable by applying the 3D substrate. The cell using the aqueous slurry and the 3D substrates for the both positive and negative showed an excellent cycle-life performance: the cell maintained more than 90% capacity



of the maximum value even at the 200th cycle. It is noteworthy that aqueous slurry based on PTFE dispersion can be applied for LiFePO<sub>4</sub> positive electrode by using the Ni–Cr 3D substrate.

The 3D substrate has high flexibilities in structure, such as thickness, porosity, and pore size. By optimizing the structure of the 3D substrate and the annealing condition, a much improvement in the lithium ion battery using alloy-based negative electrodes will be realized. Besides, this methodology also would lead to the simplification of the manufacturing process of lithium ion batteries and reduce the environmental load.

### Acknowledgments

The authors thank Fukuda Metal Foil & Powder Co. Ltd. and Mitsui Engineering & Shipbuilding Co. Ltd. for providing the alloy powder and the carbon layer deposited lithium iron phosphate, respectively. The authors also thank Mr. Yasuki Toyoshima at Osaka Institute of Technology for his assistance with the experiments and for fruitful discussion.

### References

- [1] R.A. Huggins, *J. Power Sources* 81–82 (1999) 13–19.
- [2] T. Sakai, *Electrochemistry* 71 (2003) 723–728.
- [3] K.D. Kepler, J.T. Vaughey, M.M. Thackeray, *Electrochem. Solid-State Lett.* 2 (1999) 307–309.
- [4] Y.-Y. Xia, T. Sakai, T. Fujieda, M. Wada, H. Yoshinaga, *J. Electrochem. Soc.* 148 (2001) A471–A481.
- [5] K. Wang, X. He, L. Wang, J. Ren, C. Jiang, C. Wan, *J. Electrochem. Soc.* 153 (2006) A1859–A1862.
- [6] N. Jayaprakash, N. Kalaiselvi, C.H. Doh, *J. Appl. Electrochem.* 37 (2007) 567–573.
- [7] H.-C. Shin, M. Liu, *Adv. Funct. Mater.* 15 (2005) 582–586.
- [8] Y. Yamakawa, M. Wada, T. Sakai, *Electrochemistry* 76 (2008) 203–207.
- [9] I. Matsumoto, S. Ikeyama, T. Iwaki, H. Ogawa, *Denki Kagaku* 54 (1986) 159–163.
- [10] H. Fukunaga, M. Kishimi, N. Matsumoto, T. Ozaki, T. Sakai, T. Tanaka, T. Kishimoto, *J. Electrochem. Soc.* 152 (2005) A905–A912.
- [11] M. Yao, K. Okuno, T. Iwaki, M. Kato, K. Harada, J.-J. Park, S. Tanase, T. Sakai, *Electrochem. Solid-State Lett.* 10 (2007) A56–A59.
- [12] M. Yao, K. Okuno, T. Iwaki, S. Tanase, K. Harada, M. Kato, K. Emura, T. Sakai, *J. Power Sources* 171 (2007) 1033–1039.
- [13] M. Yao, K. Okuno, T. Iwaki, M. Kato, S. Tanase, K. Emura, T. Sakai, *Electrochem. Solid-State Lett.* 10 (2007) A245–A249.
- [14] M. Yao, K. Okuno, T. Iwaki, M. Kato, K. Emura, S. Tanase, T. Sakai, *ITE Lett.* 8 (2007) 544–547.
- [15] K. Okuno, M. Yao, T. Iwaki, M. Kato, T. Awazu, S. Tanase, T. Sakai, *ITE Lett.* 8 (2007) 679–683.
- [16] M. Yao, K. Okuno, T. Iwaki, M. Kato, K. Emura, S. Tanase, T. Sakai, *J. Power Sources* 173 (2007) 545–549.
- [17] N. Hatta, T. Inaba, *Mitsui Zosen Tech. Rev.* 188 (2006) 21–25.
- [18] S. Yata, Y. Hato, H. Kinoshita, N. Ando, A. Anekawa, T. Hashimoto, M. Yamaguchi, K. Tanaka, T. Yamabe, *Synth. Met.* 73 (1995) 273–277.
- [19] Y. Idota, T. Kubota, A. Matsufuji, Y. Maekawa, T. Misayaka, *Science* 276 (1997) 1395–1397.
- [20] I.A. Courtney, J.R. Dahn, *J. Electrochem. Soc.* 144 (1997) 2045–2052.
- [21] I.A. Courtney, J.R. Dahn, *J. Electrochem. Soc.* 144 (1997) 2943–2948.
- [22] I.A. Courtney, W.R. McKinnon, J.R. Dahn, *J. Electrochem. Soc.* 146 (1999) 59–68.
- [23] H. Mukaibo, T. Sumi, T. Yokoshima, T. Momma, T. Osaka, *Electrochem. Solid-State Lett.* 6 (2003) A218–A220.
- [24] H. Mukaibo, T. Momma, T. Osaka, *J. Power Sources* 146 (2005) 457–463.
- [25] H. Yu, V. Vuorinen, J.K. Kivilahti, *J. Electron. Mater.* 36 (2006) 136–146.
- [26] C.-H. Wang, S.-W. Chen, *Metall. Mater. Trans. A* 34A (2003) 2281–2287.
- [27] J.-J. Zhang, Y.-M. Zhang, X. Zhang, Y.-Y. Xia, *J. Power Sources* 167 (2007) 171–177.